A.V. Moltasov, S.I. Motrunicz

Tests of Local Stresses in the Geometric Heterogeneity Area of Butt Welded Joints with One-Sided Excess Weld Metal

Abstract: The article is concerned with the development of analytical testing method related to stresses in stress concentration areas in butt welded joints with one-sided excess weld metal. The innovativeness of this research work consists in taking into consideration the shift of joint cross-section centres of inertia located in the excess weld metal area. The research led to the obtainment of formulas describing stresses in geometric heterogeneity areas triggered by tensile force and bending moment induced by the shift of the inertia centre. The formulas obtained in the research coincide with the results of stress-related numerical modelling. It was ascertained that an increase in eccentricity combined with the distance from the excess weld metal base could lead to greater stresses in the weld root area than those on the weld face side. The research involved the performance of fatigue tests in the high-cycle area of TIG butt welded joints of sheets made of aluminium alloy 1460. It was ascertained that in the specimens having the gentle toe (between the weld and the base material) the crack was initiated in the weld root, which was consistent with calculation-based forecast.

Keywords: butt welded joint, one-sided excess weld metal, stresses, concentration of stresses, eccentricity, fatigue cracking

DOI: *10.17729/ebis.2017.4/5*

During the one-sided butt welding of sheets, the nature of operating stress distribution could be significantly affected by bending. This is because in the above-named joints the height of excess weld metal h is similar to the thickness of joined sheets δ. The latter significantly contributes to the significant asymmetry of butt-welded joints exposed to operating loads generating stresses induced by eccentric tension. In such stress conditions, the field of normal stresses triggered by an operating tensile load is identified through the superposition of effective stresses and bending moment-induced stresses compressive in the weld face area and tensile in the weld root area. Because of the foregoing, the algebraic summation of such constituents will decrease stresses on the weld face side and increase stresses on the weld root side [1].

In work [2], the proposed formula enabling the identification of stress σr on the weld root side was the following

$$\sigma_r = P\frac{\delta + 8e}{(\delta + 2e)^2} \quad (1),$$

where P – tensile force affecting the width unit of a welded joint; δ – thickness of the

A.V. Moltasov, S.I. Motrunicz – E. O. Paton Electric Welding Institute, the National Academy of Sciences of Ukraine, Kiev

base material; e – eccentricity of tensile load application.

When analysing formula (1) it was noticed that the above-named formula did not allow for the concentration of stresses connected with the geometrical shape of the toe, e.g. the toe bend radius, being one of the primary geometrical parameters determining the degree of stress concentration [3]. According to formulas presented in work [4], an increase in stresses on the rounded surface of the toe (to satisfy equilibrium conditions in appropriate cross-sections) is compensated by a certain decrease in stresses on the weld root side. For this reason, in order to obtain a more precise assessment of stresses in the stress concentration areas in butt welded joints with one-sided excess weld metal it is necessary to take into consideration both the shift of the inertia centre and that of the concertation of stresses. The assessment of stresses in complex structured elements subjected simultaneously to tensile force and a bending moment can be performed using sufficiently effective and simple methods based on the broken line theory [5, 6].

In accordance with the above-named theory, a cut along broken line is made across point A located on the toe surface so that segment AB is perpendicular to the toe surface and has length a_0, whereas segment BC is perpendicular to the load effect line. The parameter of broken cross-section a_0 characterises the depth of notch effect and, according to publication [7], in relation to the toe is determined using the following formula:

$$a_0 = 2\sqrt{r \cdot t} \tag{2},$$

where t – toe height.

When describing the geometrical shape of the toe and the convex fragment of the excess weld metal in the form of arcs of circles being in contact with each other (Fig. 1), toe height t is expressed by toe radius r using the following formula

$$t=r\cdot(1-\cos\theta_f) \tag{3},$$

where θ_f – angle of the sector, which, in accordance with the scheme (Fig. 1) is determined by height h and width g of the excess weld metal using the following formula:

$$\theta_f = \arctan\frac{4g \cdot h}{g^2 - 4h^2} \tag{4},$$

Therefore, by replacing formula (3) taking into consideration formula (4) in formula (2), in the case under discussion the following formula is obtained

$$a_0 = 4\sqrt{2}\frac{r \cdot h}{\sqrt{g^2 + 4h^2}} \tag{5},$$

Using the same principle, the cross-section along line $A_1B_1C_1$ across point A_1 is built so that extensions of segments AB and A_1B_1 form infinitely small angle $\Delta\alpha_1$ (Fig. 2).

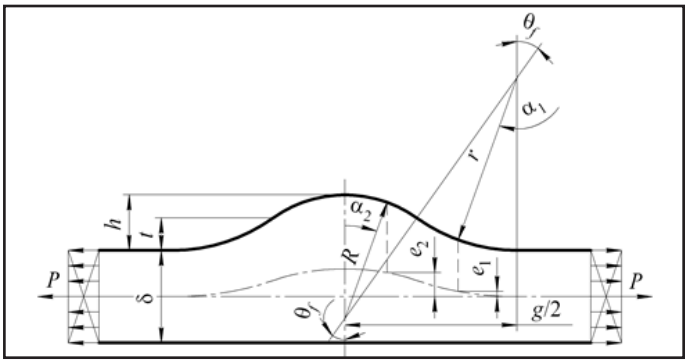

Fig. 1. Geometrical parameters of the ideal butt welded joint with one-sided excess weld metal

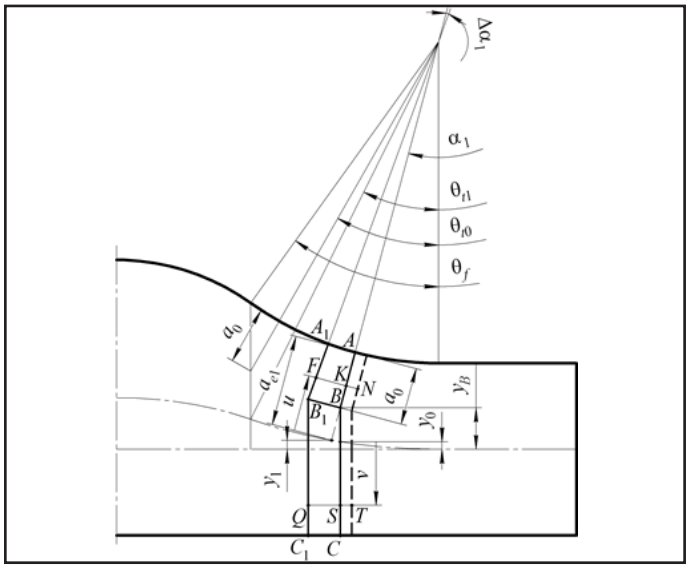

Fig. 2. Structural scheme of broken cross-sections in the stress concentration area of the butt welded joint with one-sided excess weld metal

Tension

Assuming that, because of strain, cross-section $A_1B_1C_1$ remained where it was previously and cross-section *ABC* adopted the position marked using the dashed line (Fig. 2), fibre *KF*, located at distance u from the cross-section inertia centre, gains extension *KN*, leading to the generation of normal tensile stress

$$\sigma_u^T = \frac{KN \cdot E}{\left(r + a_{e1} - u\right) \cdot \Delta\alpha_1} \quad (6),$$

as in accordance with the scheme (Fig. 2)

$KF=(r+a_{e1}-u)\cdot tg\Delta\alpha_1$

and equation $tg\Delta\alpha_1 \approx \Delta\alpha_1$ applies to infinitely small angles.

The geometric characteristic of broken cross-section a_{e_1} is determined using the following formula

$$a_{e1} = \frac{\delta - 2y_1 + 2r\left(1 - \cos\alpha_1\right)}{2\cos\alpha_1} \quad (7),$$

Value y_1 takes into consideration the distance between the load effect axis and cross-section inertia centres. If the extension of segment *AB* crosses the curve of inertia centres in its concave fragment, which is tantamount to the satisfaction of condition

$$\alpha_1 \le \theta_{t1} = \arctan\frac{2r \cdot \sin\theta_f}{\delta + r\left(1 + \cos\theta_f\right)} \quad (8),$$

$$y_1 = \frac{\left(\frac{\delta}{2} + r\right) \cdot \tan^2\alpha_1 + 2r - \sqrt{4r^2 - \delta \cdot \left(2r + \delta\right) \cdot \tan^2\alpha_1}}{4 + \tan^2\alpha_1} \quad (9),$$

However, if condition (8) is not satisfied and the extension of segment *AB* crosses the curve of inertia centres in its convex fragment, then

$$y_1 = \frac{2h - 2R + \left(r + \frac{\delta}{2}\right) \cdot \tan^2\alpha_1 - \frac{g}{2}\tan\alpha_1}{4 + \tan^2\alpha_1} + \frac{\sqrt{4R^2 - g^2 + 2g \cdot \left(R + \delta - h + 2r\right) \cdot \tan\alpha_1 + \left[2R\left(h - \delta - r\right) - \left(\delta - h\right)^2 + 4r\left(h - \delta - r\right)\right] \cdot \tan^2\alpha_1}}{4 + \tan^2\alpha_1}, \quad (10),$$

where *R* – radius of the convex fragment of the excess weld metal, which, in accordance with the adopted geometrical model (Fig. 1), is determined using the following formula

$$R = \frac{g^2 + 4h^2}{8h} - r \quad (11),$$

At the same time, fibre *QS*, located at distance *v* from the cross-section inertia centre, gains extension *ST*, leading to the generation of normal tensile stress

$$\sigma_v^T = \frac{ST}{QS} = \frac{KN \cdot \cos\alpha_1 \cdot E}{\left(r + a_0\right) \cdot \cos\alpha_1 \cdot \tan\Delta\alpha_1} = \frac{KN \cdot E}{\left(r + a_0\right) \cdot \Delta\alpha_1} \quad (12),$$

The equilibrium condition for the joint having the unitary thickness adopts the following form

$$P = \int_{a_{e1} - a_0}^{a_{e1}} \sigma_u^T du \cdot \cos\alpha_1 + \int_{-y_B + y_0}^{\delta/2 + y_0} \sigma_v^T dv \quad (13),$$

where

$$y_B = \frac{\delta}{2} + r \cdot \left(1 - \cos\alpha_1\right) - a_0 \cdot \cos\alpha_1 \quad (14),$$

Parameter y_0 also takes into consideration the distance between the load effect axis and cross-section inertia centres. If segment *BC* crosses the curve of inertia centres in its concave fragment, which is tantamount to the satisfaction of condition

$$\alpha_1 \le \theta_{t0} = \arcsin\frac{r \cdot \sin\theta_f}{r + a_0} \quad (15),$$

$$y_0 = \frac{1}{2}\left(r - \sqrt{r^2 - \left(r + a_0\right)^2 \cdot \sin^2\alpha_1}\right) \quad (16),$$

However, if condition (15) is not satisfied and segment *BC* crosses the curve of inertia centres

in its convex fragment, then

$$y_0 = \frac{1}{2}\left(h - R + \sqrt{R^2 - \left(\frac{g}{2} - \left(r + a_0 \right) \sin \alpha_1 \right)^2} \right) \quad (17).$$

Entering the formulas describing stresses (6) and (12) in equilibrium equation (13), after integration the following formula is obtained

$$\frac{P}{T_0} = \frac{KN \cdot E}{\Delta \alpha_1} \quad (18).$$

where T_0 – geometric characteristic of the broken cross-section in relation to extension, which, along with the change in cross-sections, changes in accordance with the following principle

$$T_0 = \cos \alpha_1 \cdot \ln \frac{r + a_0}{r} + \frac{\delta + 2 y_B}{2\left(r + a_0 \right)} \quad (19).$$

After entering term (18) in equations (6) and (12), the following correlation between tensile force P and stresses on segment AB

$$\sigma_u^T = \frac{P}{\left(r + a_{e1} - u \right) \cdot T_0} \quad (20)$$

and BC

$$\sigma_v^T = \frac{P}{\left(r + a_0 \right) \cdot T_0} \quad (21)$$

respectively is obtained.

The analysis of formulas (20) and (21) reveals that, along segment BC, stress is constant across the entire thickness changing only in relation to changes in the cross-section. For this reason, in cases of tensile loads, the stresses on the weld root side are determined using equation (21), where stress along segment AB changes in accordance with a hyperbolic function and reached a maximum on the toe surface when $u = a_{e1}$. Then, in cases of tensile loads, the stresses in the weld face area are determined using the following formula

$$\sigma_f^T = \frac{P}{r \cdot T_0} \quad (22).$$

The obtained formulas apply to the case when $a_0 \le a_{e1}$, i.e. segment AB does not intersect the curve of inertia centres. If the segment did intersect the above-named curve, then, in terms (12)-(14) it would be necessary to assume that $a_0 = a_{e1}$, and, in term (13) that $y_0 = y_1$. In such a case, the lower limits in both integrals (13) transform into zero and the geometrical characteristic of the broken cross-sections in conditions of tension T_0 should be replaced with the following characteristic

$$T_1 = \cos \alpha_1 \cdot \ln \frac{r + a_{e1}}{r} + \frac{\delta + 2 y_1}{2\left(r + a_{e1} \right)} \quad (23),$$

whereas the stresses induced by the tensile load in the weld face and weld root areas will be determined using the formulas

$$\sigma_f^T = \frac{P}{r \cdot T_1} \quad (24)$$

and

$$\sigma_r^T = \frac{P}{\left(r + a_{e1} \right) \cdot T_1} \quad (25)$$

respectively.

Bending

As mentioned before, in addition to axial tension-induced stresses, the segment with one-sided excess weld metal in the butt welded joint, is also subjected to bending stresses triggered by bending moment M, which, according to work [2] is determined using the following formula

$$M = P \cdot e_1 \quad (26),$$

where e_1 – eccentricity of tensile force application on the concave segment of excess weld metal, which, in accordance with the adopted geometrical model (Fig. 1) changes in accordance with the following principle

$$e_1 = \frac{r\left(1 - \cos \alpha_1 \right)}{2} \quad (27).$$

Assuming that because of bending, cross-section $A_1B_1C_1$ remained in the same area and cross-section ABC was turned through small angle $\Delta\gamma$ and adopted the position marked with the dashed (Fig. 3), fibre KF, located at distance u from the cross-section inertia centre, gains extension KN, leading to the generation of normal tensile stress

$$\sigma_u^B = \frac{\left(\frac{y_B - y_0}{\cos\alpha_1} + u - a_{e1} + a_0\right)\Delta\gamma \cdot E}{\left(r + a_{e1} - u\right)\cdot\Delta\alpha_1} \quad (28),$$

as in accordance with the schemes (Fig. 2 and Fig. 3)

$$KN = \frac{y_B - y_0}{\cos\alpha_1}\tan\Delta\gamma + \left(u - a_{e1} + a_0\right)\cdot\tan\Delta\gamma$$

At the same time, fibre QS, located at distance v from the cross-section inertia centre, contracts by quantity ST, leading to the formation of normal compressive stress

$$\sigma_v^B = \frac{v\cdot\Delta\gamma\cdot E}{\left(r + a_0\right)\cdot\Delta\alpha_1\cdot\cos\alpha_1} \quad (29).$$

The equilibrium condition for the joint having the unitary thickness adopts the following form

$$M = \int_{a_{e1}-a_0}^{a_{e1}} \sigma_u^B \cdot \left(\frac{y_B - y_0}{\cos\alpha_1} + u - a_{e1} + a_0\right) du + \int_{-y_B+y_0}^{\delta/2+y_0} \sigma_v^B \cdot v dv \quad (30).$$

Entering the formulas describing stresses (28) and (29) in equilibrium equation (30), after integration the following formula is obtained

$$\frac{M}{B_0} = \frac{\Delta\gamma\cdot E}{\Delta\alpha_1} \quad (31),$$

where B_0 –geometric characteristic of the broken cross-section in relation to bending, which, along with the change in cross-sections, changes in accordance with the following principle

$$B_0 = \frac{\left(y_B - y_0 - \left(a_{e1} - a_0\right)\cos\alpha_1\right)^2}{\cos^2\alpha_1}\cdot\ln\frac{r + a_0}{r} + \left(r + a_{e1}\right)^2\ln\frac{r + a_0}{r} - a_0\left(r + 2a_{e1}\right) + \frac{a_0^2}{2} +$$
$$+\frac{2\left(y_B - y_0 - \left(a_{e1} - a_0\right)\cos\alpha_1\right)}{\cos\alpha_1}\cdot\left[\left(r + a_{e1}\right)\ln\frac{r + a_0}{r} - a_0\right] + \frac{\left(y_B - y_0\right)^3 + \left(\frac{\delta}{2} + y_0\right)^3}{3\left(r + a_0\right)\cos\alpha_1}. \quad (32)$$

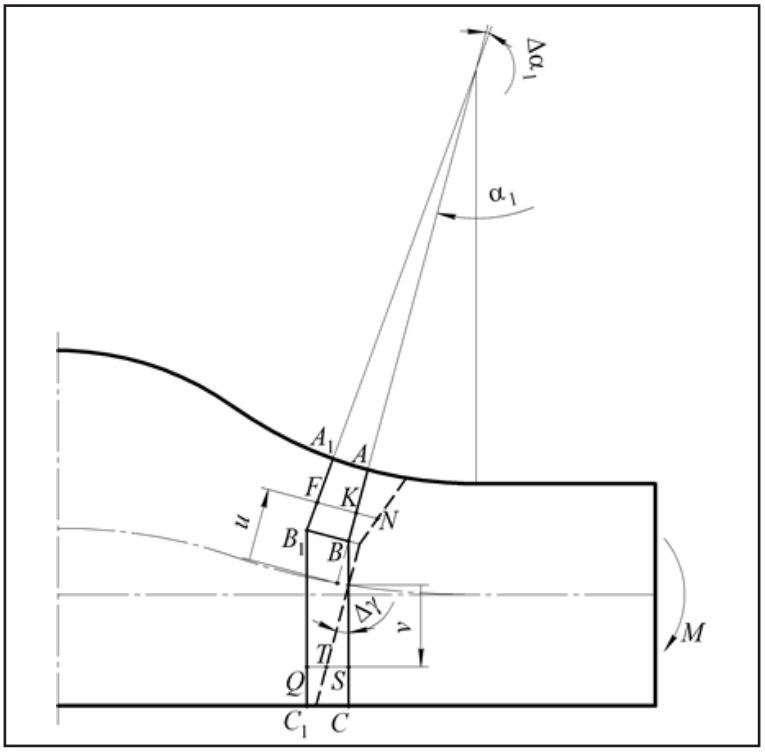

Fig. 3. Rotation of the broken cross-section during the bending of the butt welded joint

After entering term (31) in equations (28) and (29), the following correlation between bending moment P and stresses on segment *AB*

$$\sigma_u^B = \frac{M\left(\frac{y_B - y_0}{\cos\alpha_1} + u - a_{e1} + a_0\right)}{\left(r + a_{e1} - u\right)\cdot B_0} \tag{33}$$

and *BC*

$$\sigma_v^B = \frac{M\cdot v}{\left(r + a_0\right)\cdot B_0\cdot\cos\alpha_1} \tag{34}$$

respectively is obtained.

By substituting $u = a_{e1}$ in formula (33), the bending-induced stress affecting the weld face is obtained

$$\sigma_f^B = \frac{M\left(\frac{y_B - y_0}{\cos\alpha_1} + a_0\right)}{r\cdot B_0} \tag{35}$$

The bending-induced stress affecting the weld root is obtained by substituting $v = y_0 + \delta/2$ in formula (34), then

$$\sigma_r^B = \frac{M\cdot\left(\delta + 2y_0\right)}{2\left(r + a_0\right)\cdot B_0\cdot\cos\alpha_1} \tag{36}$$

The obtained formulas apply to the case when $a_0 \le a_{e1}$, but if the above-presented condition is not satisfied, in terms (28)-(30) it should be assumed that $a_0 = a_{e1}$ and $y_0 = y_1$, then the geometrical characteristic of broken cross-sections in conditions of bending B_0 should be replaced with the following characteristic

$$B_1 = \left(r + a_{e1}\right)^2 \ln\frac{r + a_{e1}}{r} - a_{e1}\left(r + 2a_{e1}\right) + \frac{a_{e1}^2}{2} + \frac{\left(\frac{\delta}{2} + y_1\right)^3}{3\left(r + a_{e1}\right)\cos\alpha_1} \tag{37},$$

whereas the stresses induced by bending in the weld face and weld root areas will be determined using the formulas

$$\sigma_f^B = \frac{a_{e1}\cdot M}{r\cdot B_1} \tag{38}$$

and

$$\sigma_r^B = \frac{\left(\delta + 2y_1\right)\cdot M}{2\left(r + a_{e1}\right)\cdot B_1\cdot\cos\alpha_1} \tag{39}$$

respectively.

Exemplary application in calculations

An example will involve the calculation of stresses in the MIG butt welded joints made of 1.8 mm thick aluminium alloy 1460 (Fig. 4) with the known parameters of height *h* and width *g* of excess weld metal (Table 1).

The data presented in Table 1 reveal that in cases of all welded joints $a_{e1}(\theta_f) < a_0$. As a result, within the entire range of the change in α_1 allowing for formulas (26) and (27), the total stresses in the weld face will be identified as the difference between the tensile stresses (24) and

Table 1. Geometrical parameters of the excess weld metal in the MIG butt welded joints made of 1.8 mm thick aluminium alloy 1460

Specimen no.	Width of excess weld metal *g*, mm	Height of excess weld metal *h*, mm	Sector angle θ_f, °	Toe radius *r*, mm	Concentrator depth a_0, mm	$a_{e1}(\theta_f)$, mm
1	7.0	0.6	19.5	2.75	1.31	0.98
2	7.3	0.6	19	2.85	1.31	0.98
3	6.9	0.8	26	2.12	1.35	1.01
4	6.6	0.6	20.6	2.62	1.33	0.99
5	6.8	0.8	26.5	2.08	1.35	1.02
6	6.8	0.6	20	2.70	1.33	0.98
7	6.6	0.6	20.6	2.62	1.33	0.99

Note: The toe radius was determined on the basis of the graphic correlation between the radius and angle of the sector [8].

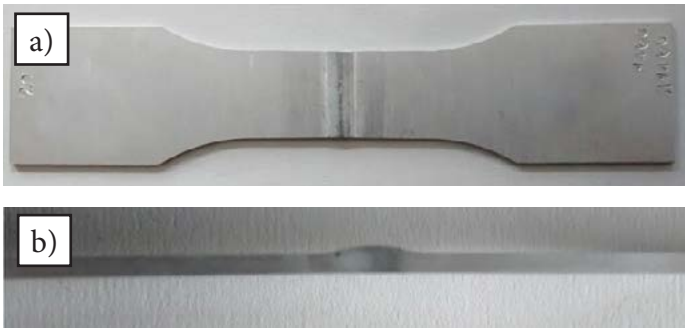

Fig. 4. Specimens used in the tests involving the MIG butt welded joints made of aluminium alloy 1460: a) outside view; b) welded joint profile

the bending moment-induced stresses (38) using the following formula

$$\sigma_f^{\Sigma} = P\left(\frac{1}{r \cdot T_1} - \frac{a_{e1}\left(1-\cos\alpha_1\right)}{2B_1}\right) \quad (40),$$

whereas the total stresses in the weld root will be determined as the difference between the tensile stresses (25) and the bending moment-induced stresses (39) using the following formula

$$\sigma_r^{\Sigma} = \frac{P}{r + a_{e1}}\left(\frac{1}{T_1} + \frac{r\left(\delta + 2y_1\right)\left(1-\cos\alpha_1\right)}{4B_1 \cdot \cos\alpha_1}\right) \quad (41).$$

It is known that along with a decrease in the toe radius *r* the concentration of stresses at the base of the one-sided excess weld metal increases [9]. Therefore, it can be presumed that the above-named level will reach its maximum in specimen no. 5, and minimum in specimen no. 2 (Table 1). For this reason, the diagrams of the stresses in the weld face and weld root areas of the joints (Fig. 5) are based on formulas (40) and (41) respectively.

The analysis of the presented distributions revealed that an increase in the toe radius from 2.08 to 2.85 mm decreased the maximum stress in the weld face area from 1.31 to 1.23. In cases of the remaining joints, the above-named stress values were intermediate (Table 2). In addition, it could be noticed in the cross-sections corresponding to the concave fragment of the excess weld metal, the stresses in the weld root were higher than those in the weld face area.

Because of the fact that formulas (40) and (41) can only be applied when calculating stresses in the concave fragment of the excess weld metal, to obtain the complete image of stress distribution, including the cross-sections corresponding to the convex fragment of the excess weld metal, it was necessary to perform the computer-aided FEM modelling of stress fields in related specimens (Fig. 6).

Table 2. Calculation results related to maximum stresses in the weld face and weld root areas of the butt welded joints made in aluminium alloy 1460

Specimen no.	1	2	3	4	5	6	7
Toe radius (r), mm	2,75	2,85	2,12	2,62	2,08	2,70	2,62
Maximum stress in the weld face area $\sigma_f^{max}/\sigma_{nom}$	1,24	1,23	1,30	1,25	1,31	1,24	1,25

Note: σ_{nom} – nominal tress distant from the excess weld metal.

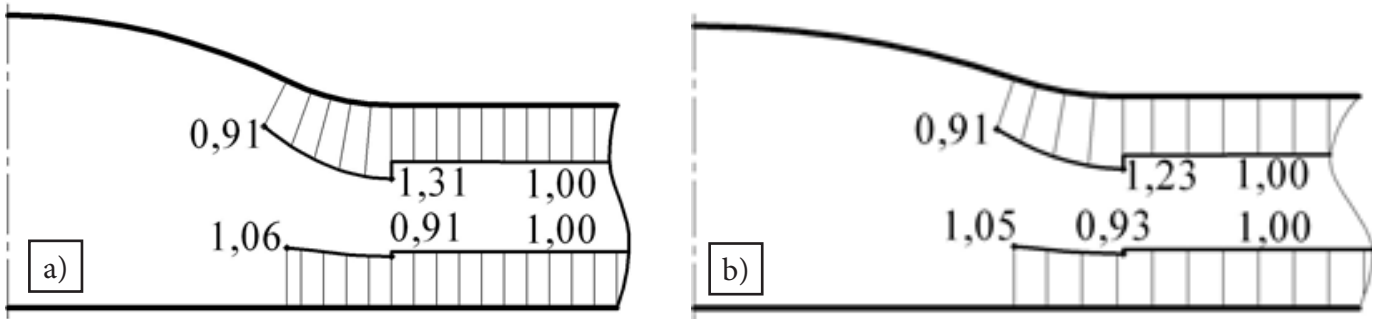

Fig. 5. Distribution of stresses in the weld root and weld face areas of specimen: a) no. 5; b) no. 2

The comparative analysis of the distributions (Fig. 5) and fields of stresses (Fig. 6) revealed that, in the areas corresponding to the concave fragment of the excess weld metal coincided satisfactorily both in terms of quantity and quality. As was the case with specimen no. 5, the difference between the calculated values at the base of the excess weld metal amounted to 0.76%, whereas in relation to specimen no. 2 the difference amounted to 0.73%.

It could also be noticed that in specimen no. 5 the stresses at the base of the excess weld metal were significantly higher than those in the weld root, whereas in specimen no. 2 the stresses were the same (Fig. 6). Therefore, in accordance with Table 2, the fatigue crack in specimens no. 3 and no. 5 would probably be formed at the base of the excess weld metal, whereas in cases of the remaining specimens the formation of fatigue cracks could be expected both on the weld face and weld root side, which was confirmed by the fatigue test results in high-cycle area (Fig. 7).

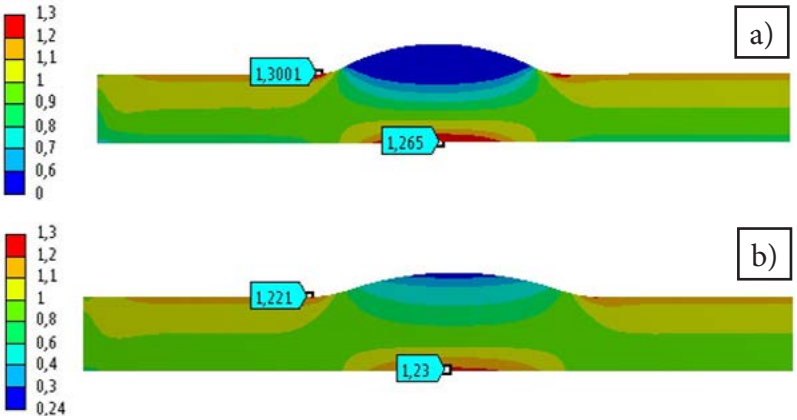

Fig. 6. Fields of stresses in specimens: a) no. 5; b) no. 2

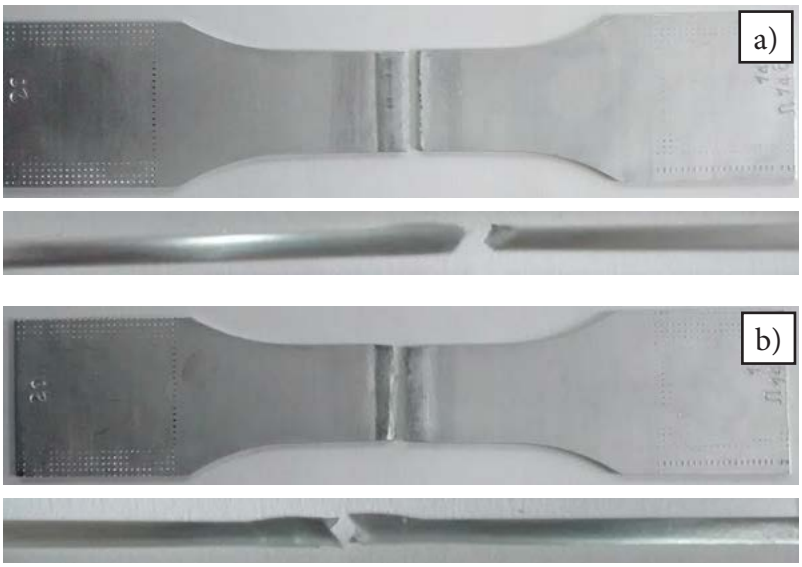

Fig. 7. Fatigue crack of specimens made of aluminium alloy 1460: a) fatigue crack was formed at the base of the excess weld metal on the weld face side; b) fatigue crack was formed in the weld root

Conclusions

1. The broken cross-section theory was used to develop an analytical method concerning tests of local stresses in the geometric heterogeneity areas of but welded joints with one-sided excess weld metal taking into consideration the shift of cross-sectional inertia centres located in the excess weld metal area in relation to the tensile load axis.

2. The research resulted in the development of formulas describing stress changes in the geometric heterogeneity area, both along the shape line and deep inside the butt welded joints with one-sided excess weld metal. The foregoing enabled the description of stresses in the weld face and weld root areas.

3. The FEM-based numerical modelling of stresses present during the tension of MIG butt welded joints made of aluminium alloy 1460 with one-sided excess weld metal revealed that the size and nature of stress distribution obtained using the analytical and numerical methods were nearly the same. In addition, it was proved that the bending stresses in the specimens with the relatively gentle toe could trigger the formation of fatigue cracks in the weld root, which was confirmed by the fatigue test results in the high-cycle area.

References

[1] Цумарев Ю.А:. *Влияние асимметрии односторонних стыковых швов на распределение напряжений в сварном соединении*. Сварка и диагностика, 2010,

no. 5, pp. 24–27.

[2] Цумарев Ю.А.: *Влияние внецентренного растяжения на напряженное состояние стыкового сварного соединения.* Сварочное производство, 2010, no. 6, pp. 6–10.

[3] Кныш В.В.: *Повышение сопротивления усталости тонколистовых сварных соединений алюминиевых сплавов высокочастотной проковкой* /В.В. Кныш, И.Н. Клочков, М.П. Пашуля, С.И. Мотрунич/, Автоматическая сварка, 2014, no. 5, pp. 22–29.

[4] Молтасов А.В.: *Применение метода неплоских сечений к определению напряжений в зонах концентрации, вызванной усилением стыкового сварного соединения*. Проблемы прочности, 2013, no. 1, pp. 159–167.

[5] Верховский А.В.: *Гипотеза ломаных сечений и её применение к расчёту стержней сложной конфигурации*. Известия ТПИ, 1947, no.1 (61), pp. 3–46.

[6] Молтасов А.В.: *Инженерный метод расчёта коэффициента концентрации напряжений в нахлёсточном сварном соединении при растяжении и изгибе.* /А.В. Молтасов, И.Н. Клочков, В.В. Кныш/, Вісник НТУУ "КПІ": серія "Машинобудування", 2013, no. 3, pp. 150–157.

[7] Верховский А.В.: *Определение напряжений в опасных сечениях деталей сложной формы. Метод неплоских сечений.* /А.В. Верховский, В.П. Андронов, В.А. Ионов, О.К. Лупанова, В.И. Чевкинов/, Москва: Машгиз, 1958, p. 147

[8] Березовский Б.М.: *Особенности формирования зоны перехода от усиления стыкового шва к основному металлу.* /Б.М. Березовский, В.А. Стихин/, Вопросы сварочного производства, 1981, no.266, pp. 99–106.

[9] Neuber H.: Kerbspannungslehre: *Theorie der Spannungskonzentration Genaue Berechnung der Festigkeit.* Vierte Verlag – Berlin: Springer-Verlag Berlin Heidelberg, 2001, 326 – (Klassiker der Technik).